



Synthesis and mechanical properties of carbon nanotube/diamond-like carbon composite films

Kinoshita, Hiroshi

Kume, Ippei

Sakai, Hirokazu

Ohmae, Nobuo

(Citation)

Diamond and Related Materials, 16(11):1940-1944

(Issue Date)

2007-11

(Resource Type)

journal article

(Version)

Accepted Manuscript

(URL)

<https://hdl.handle.net/20.500.14094/90000922>



Title

Synthesis and mechanical properties of carbon nanotube/diamond-like carbon composite films

Authors:

Hiroshi Kinoshita*, Ippei Kume, Hirokazu Sakai, Nobuo Ohmae

Keywords:

Carbon nanotube; Diamond like carbon; Composite film; Toughening; Hardness; Friction

Full postal address of all co-authors

**Department of Mechanical Engineering, Faculty of Engineering, Kobe University,
ZIP code: 657-8501 Rokkodai 1-1, Nada-Ku, Kobe, JAPAN**

***corresponding author**

Tel&Fax: +81-78-803-6126

E-mail address: kinohiro@people.kobe-u.ac.jp

Abstract

Diamond-like carbon (DLC) coatings were successfully deposited on carbon nanotube (CNT) films with CNT densities of $1 \times 10^9/\text{cm}^2$, $3 \times 10^9/\text{cm}^2$, and $7 \times 10^9/\text{cm}^2$ by a radio frequency plasma-enhanced chemical vapor deposition (CVD). The new composite films consisting of CNT/DLC were synthesized to improve the mechanical properties of DLC coatings especially for toughness. To compare those of the CNT/DLC composite films, the deposition of a DLC coating on a silicon oxide substrate was also carried out. A dynamic ultra micro hardness tester and a ball-on-disk type friction tester were used to investigate the mechanical properties of the CNT/DLC composite films. A scanning electron microscopic (SEM) image of the indentation region of the CNT/DLC composite film showed a triangle shape of the indenter, however, chippings of the DLC coating were observed in the indentation region. This result suggests the improvement of the toughness of the CNT/DLC composite films. The elastic modulus and dynamic hardness of the CNT/DLC composite films decreased linearly with increasing their CNT density. Friction coefficients of all the CNT/DLC composite films were close to that of the DLC coating.

1. Introduction

Diamond-like carbon (DLC) coatings, which have the large fractions of sp^3 bondings, have also good mechanical properties, including high hardness and low friction coefficients. However, DLC coatings have less toughness [1]. Since film toughness is as important as hardness for practical use, toughness of DLC coatings should be improved.

Carbon nanotubes (CNTs) have cylinder structure of graphene sheets (sp^2 bonding network) with diameters of less than a few tens of nm [2]. For their structure, CNTs have significant mechanical properties, such as high elastic modulus, large elastic strain, and high toughness. It has been reported that in spite of the high stiffness of carbon nanotubes (having a Young's modulus of more than 1 TPa), they can be elastically deformed under large lateral displacement [3-5]. Thus, CNTs are used to reinforce nanomaterials as fibers, or to improve tribological properties of composite materials [1,6,7].

In this study, we report synthesis of CNT/DLC composite films in three steps; (1) formations of Fe nanoparticles on silicon oxide wafers, (2) growths of CNT films, and (3) deposits of DLC coatings. Scanning electron microscopy (SEM) and transmission electron microscopy (TEM) were used to observe microstructures of the CNT/DLC composite films. The mechanical properties of the CNT/DLC composite films were investigated by a dynamic ultra micro hardness tester and a ball-on-disk type friction tester. To estimate the toughness, the indent regions were observed by SEM.

2. Experiment

The synthesis of CNT/DLC composite films was carried out in three steps as schematically shown in Fig. 1.

Step 1 (formation of Fe nanoparticles): when using CVD, metal nanoparticles are necessary for CNTs to nucleate and grow [8,9]. In this study, H-terminated Si(001) wafers formed by HF dip were used as substrates. Silicon oxide layers with approximately 30 nm thick were formed on H-terminated Si(001) wafers by thermal oxidation with 760 Torr O_2 gas at a temperature of 800°C for 2 h. Catalytic layers of Fe

with a thickness of 0.5 nm were then deposited on the substrates using a vacuum evaporation. Annealing treatments of the substrates were conducted at 800°C in the flowing H₂, providing Fe nanoparticles with a size of below 100 nm. Annealing times were varied from 10 to 30 min to obtain different densities of the Fe nanoparticles.

Step 2 (growth of CNT films): CNT films were grown by a microwave plasma-enhanced CVD apparatus. The details of the apparatus were described elsewhere [10]. A mixture of CH₄ and H₂ gases and a microwave plasma at 2.45 GHz and 500 W were used. The substrate temperature was kept at 700 °C during the deposition process. The time for deposition of CNT films was set for 20 s.

Step 3 (deposition of DLC coatings): A radio frequency (13.56 MHz) plasma-enhanced CVD apparatus (Nippon ITF Inc.) was used for DLC deposits. The plasma input power was 1000 W. A mixture of CH₄ and H₂ gases was used. The deposit time was 1 h and the DLC coatings deposited on CNT films were approximately 1 μm thick.

We successfully prepared three CNT/DLC composite films with different CNT densities by varying annealing time in Step 1. A DLC coating deposited directly on a silicon oxide substrate was also prepared as a reference to CNT/DLC composite films.

SEM was used to observe the densities and lengths of CNT films, surface morphologies of CNT/DLC composite films, and indented areas of indentation tests. TEM was used to determine the microstructure of individual CNTs and the inner parts of CNT/DLC composite films. Dynamic hardness and elastic modulus of CNT/DLC composite films were measured by a dynamic ultra micro hardness tester. The dynamic hardness defined by DHT115 was employed [11]. The loading conditions were a constant loading rate of 1.42 mN/s, a maximum load of 5 mN, and a holding time of 2 s

followed by unloading. The frictional tests of CNT/DLC composite films were carried out with a ball-on-disk friction tester. SUS304 ball with a diameter of 1 mm was used. Loads were varied till 2 N with a sliding speed of 0.1 mm/s at 20 °C with a humidity of 25 %.

3. Results and discussion

3.1. Synthesis of CNT/DLC composite films

Figs. 2 (a)-(c) show the SEM images of CNT films with CNT densities of $1 \times 10^9/\text{cm}^2$, $3 \times 10^9/\text{cm}^2$, and $7 \times 10^9/\text{cm}^2$, in which annealing times of the Fe particles were 10, 20, and 30 min, respectively. CNT lengths were varied from 0.3 to 0.5 μm . TEM images (not shown) revealed that the growth of multiwalled CNTs were found and the diameters of CNTs were from 20 to 50 nm. After the synthesis of the CNTs on the substrates, DLC were deposited on the CNTs. Figs. 2 (d)-(f) show SEM images of the CNT/DLC composite films (after DLC depositions) with the initial CNT densities of $1 \times 10^9/\text{cm}^2$, $3 \times 10^9/\text{cm}^2$, and $7 \times 10^9/\text{cm}^2$, respectively. The surfaces after the DLC depositions are flat and no CNTs were observed on the surfaces, indicating that the DLC deposited over the tops of the CNT films. Fig. 3 represents the TEM image of the inner parts of the CNT/DLC composite film with the CNT density of $7 \times 10^9/\text{cm}^2$. CNT was shown in the arrow in Fig. 3. It is observed that DLC adhered to the CNT tightly.

DLC coating was deposited on a CNT film with a CNT length of 2 μm and a CNT density of $1 \times 10^{10}/\text{cm}^2$. The CNT film was obtained from Fe catalytic layer with a thickness of 5 nm and the annealing time of 30 min. The other conditions for the CNT growth and the DLC deposit were not changed. Figs.4 (a) and (b) represent the SEM images of the CNT film and the film after the DLC coatings, respectively. As shown in

Fig. 4 (b), the DLC coating was only deposited on the top part of the CNT film. It appears that entire deposition of DLC is not possible unless the CNTs are short and have low density.

3.2. Mechanical properties of CNT/DLC composite films

Fig. 5 shows the dynamic hardness (DHT115) of the CNT/DLC composite films and DLC coating as a function of the density of the CNTs. The dynamic hardness decreases linearly with increasing the density. The relationship between the elastic modulus of the CNT/DLC composite films and the CNT densities is shown in Fig. 6. The elastic modulus also decreases linearly with increasing the density. Dynamic hardness and elastic modulus of the DLC coating measured were 1227 and 230 GPa, respectively. These results show that CNTs cause the decrease of the dynamic hardness and the elastic modulus of DLC coatings. Although individual CNTs have strong mechanical properties, CNT films were soft because of their fiber structure. Generally dynamic hardness and elastic modulus of fiber materials are thought to be proportional to their density. Considering the CNT densities, the dynamic hardness and the elastic modulus of the CNT films in the CNT/DLC composite films would be less than the values of the DLC coating shown above (0.25 and 350 MPa). Since the DLC coating had much higher hardness and elasticity than CNT films, it is concluded that the increase of the CNT density in the CNT/DLC composite film causes the decrease of their dynamic hardness and elastic modulus.

Figs. 7 (a) and (b) show the SEM images of indentation regions of the DLC coating and the CNT/DLC composite films with the CNT density of $7 \times 10^9/\text{cm}^2$. It is found that the DLC coating was chipped and the triangle shape of the indenter is not

clearly confirmed. The chipping the DLC coating may result from the less toughness. On the other hand, the triangle shape is observed for the CNT/DLC composite film. These results imply that toughness increases with adding CNTs in DLC coatings.

Friction forces were found to be proportional to applied forces for all the three composite films, and thus friction coefficients were calculated from the linear relationships. Fig. 8 represents the relationships between the friction coefficient of the CNT/DLC composite films and the CNT density. The friction coefficients are approximately 0.23 for all samples. Since no wear track was observed in the friction test, the ball contacted only with the DLC coatings on the surfaces of the CNT/DLC composite films. Therefore, friction coefficients of all the CNT/DLC composite films were close to that of the DLC coating.

4. Summary

The synthesis of the CNT/DLC composite films was attempted. SEM and TEM observations showed that low density and short length of CNTs are required to synthesize CNT/DLC composite films. A SEM image of the indentation region of the CNT/DLC composite film suggests the improvement of the toughness of the CNT/DLC composite films. The toughness is increased in the CNT/DLC composite thin film. The dynamic hardness and elastic modulus of the CNT/DLC composite films decreases linearly with increasing the CNT density, because the DLC coating had much higher hardness and elasticity than CNT films. The increase of the CNT density did not affect the friction coefficient of the CNT/DLC composite films.

References

- [1] S. Zhang, D. Sun, Y. Fu, H. Du, Surface and Coatings Technology 198 (2005) 2.
- [2] S. Iijima., Nature 354 (1991) 56.
- [3] J. -P. Salvetat-Delmotte and A. Rubio, Carbon 40 (2002) 1729.
- [4] E. W. Wong, P. E. Sheehan, and C. M. Lieber., Science 277 (1997) 1971.
- [5] H.J.Qi, K. B. K. Teo, K. K. S. Lau, M. C. Boyce, W. I. Milne, J. Robertson, and K. K. Gleason, Journal Of The Mechanics And Physics Of Solids 51 (2003) 2213.
- [6] W.X. Chen, J.P. Tu, L.Y. Wang, H.Y. Gan, Z.D. Xu, X.B. Zhang, Carbon 41 (2003) 215.
- [7] D.S. Lim, J.W. An, H.J. Lee, Wear 252 (2002) 512.
- [8] M. Chhowalla, K.B.K. Teo, C. Ducati, N.L. Rupesinghe, G.A.J. Amaratunga, A.C. Ferrari, D. Roy, J. Robertson, W.I. Milne, Journal Applied Physics 90 (2001) 5308.
- [9] P.H. Maun, C.H. Emmenegger, A. Züttel C.H. Nutzenadel, P. Sudan, L. Schlapbach,., Carbon 40 (2002) 1339.
- [10] H. Kinoshita, I. Kume, H. Sakai, M. Tagawa, N. Ohmae, Carbon 42 (2004) 2753.
- [11] Y. Fukumiya, Y. Haga, O. Nittono, Materials Science and Engineering A 312 (2001) 248.

Figure Captions

- Fig. 1 Schematic of the three step synthesis of CNT/DLC composite film. Step1; formation of Fe nanoparticles, Step2; growth of CNT films, and Step3; deposition of DLC coatings.
- Fig. 2 SEM images of the CNT films with the CNT densities of (a) $1 \times 10^9/\text{cm}^2$, (b) $3 \times 10^9/\text{cm}^2$, and (c) $7 \times 10^9/\text{cm}^2$ (before the DLC depositing) and (d)-(f) the CNT/DLC composite films corresponding to (a)-(c).
- Fig. 3 TEM image of the inner part of the CNT/DLC composite with the CNT density of $7 \times 10^9/\text{cm}^2$. CNT is shown by the arrow.
- Fig. 4 SEM images of the CNT film with the CNT length of $2 \mu\text{m}$ and the density of $1 \times 10^{10}/\text{cm}^2$ (a) before and (b) after the DLC deposition.
- Fig. 5 Dynamic hardness of the CNT/DLC composite films as a function of the CNT density of the CNT/DLC composite films. Zero CNT density indicates the DLC coating.
- Fig. 6 Relationship between elastic modulus of the CNT/DLC composite films. Zero CNT density indicates the DLC coating.
- Fig. 7 SEM images of the indentation region of (a) the DLC coating and (b) the CNT/DLC composite film with the CNT density of $7 \times 10^9/\text{cm}^2$.
- Fig. 8 Friction coefficients of the CNT/DLC composite films as a function of the density of CNTs. Zero CNT density indicates the DLC coating.

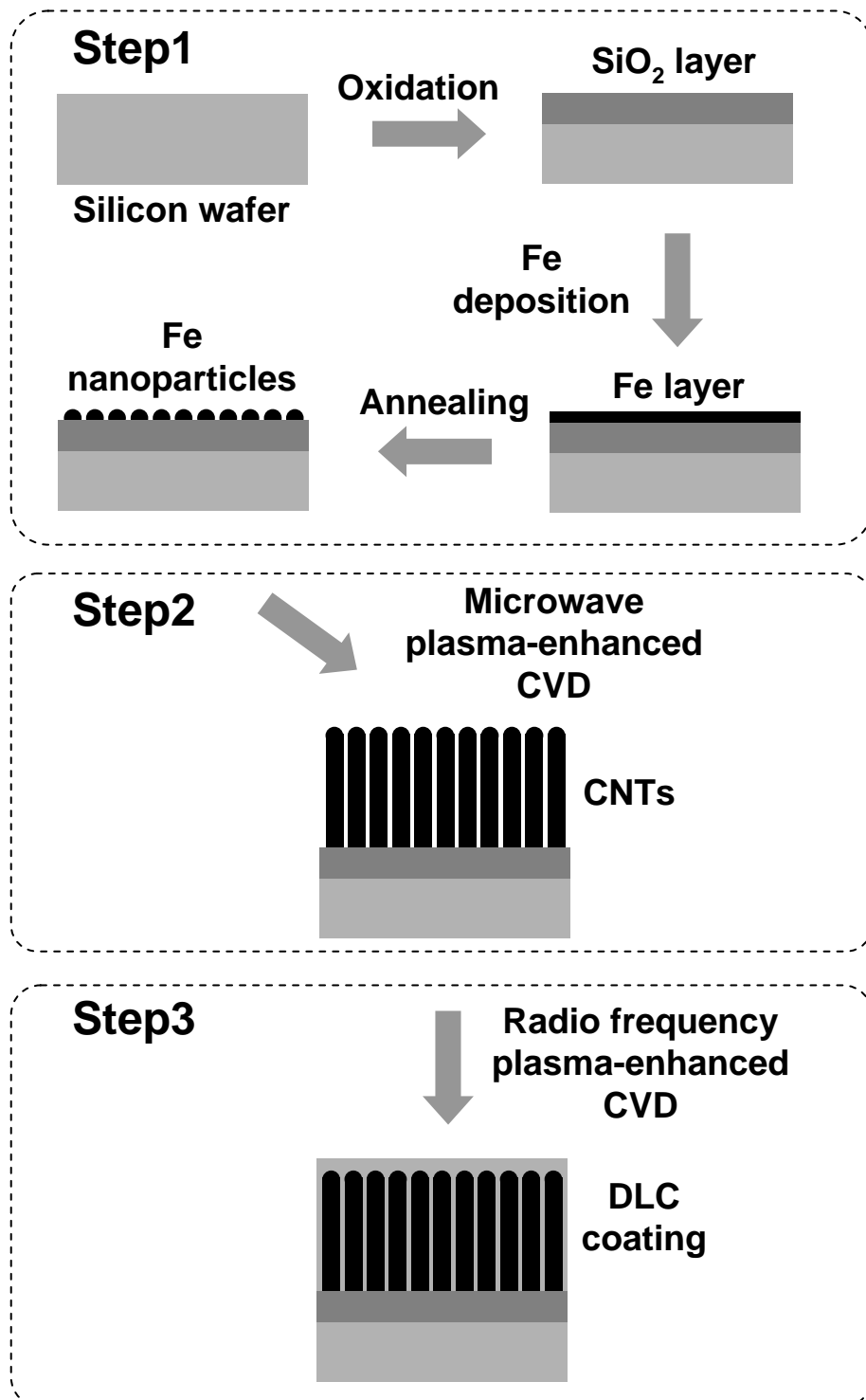


FIG.1. Kinoshita et al.

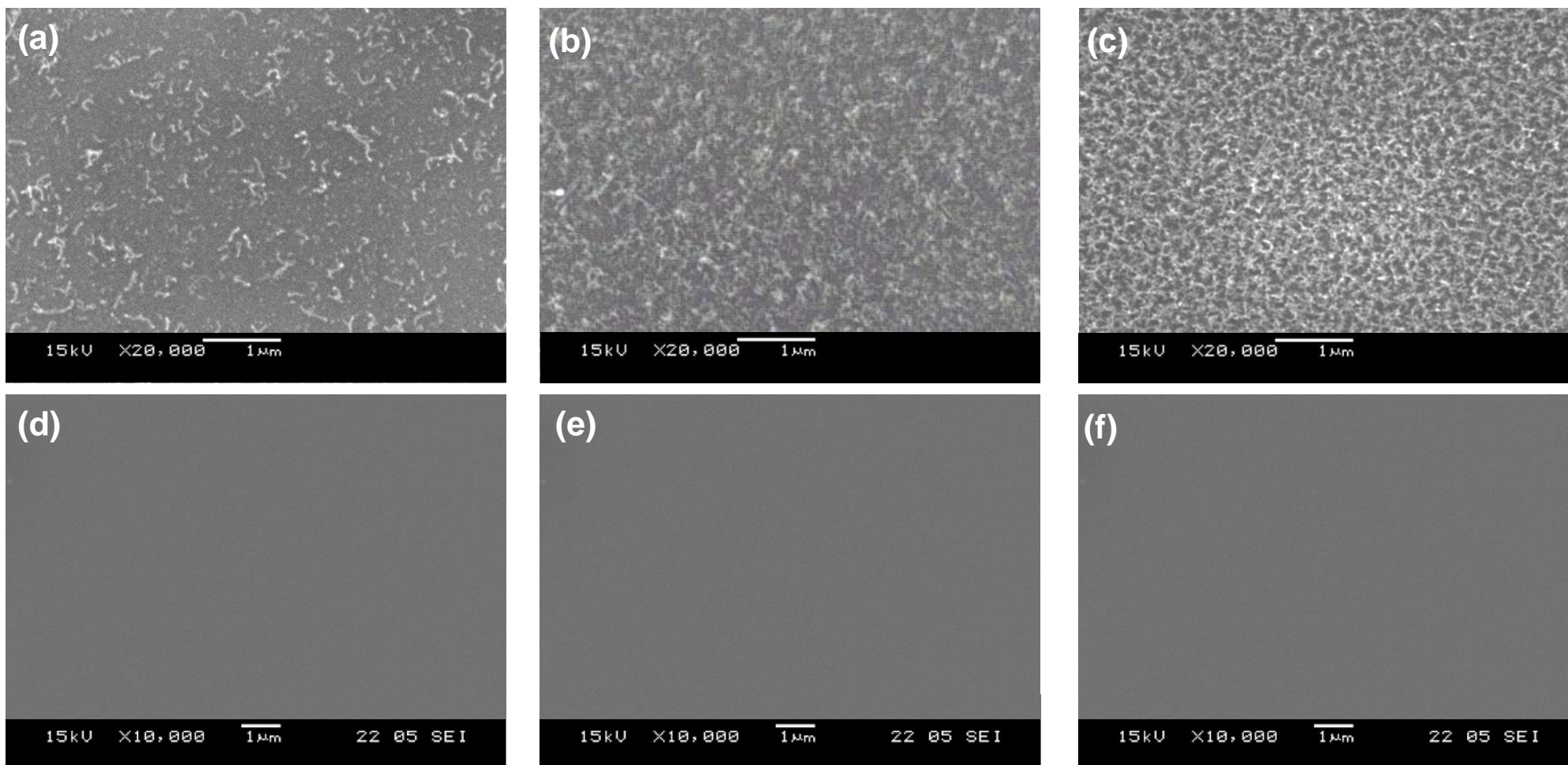


FIG.2. Kinoshita et al.

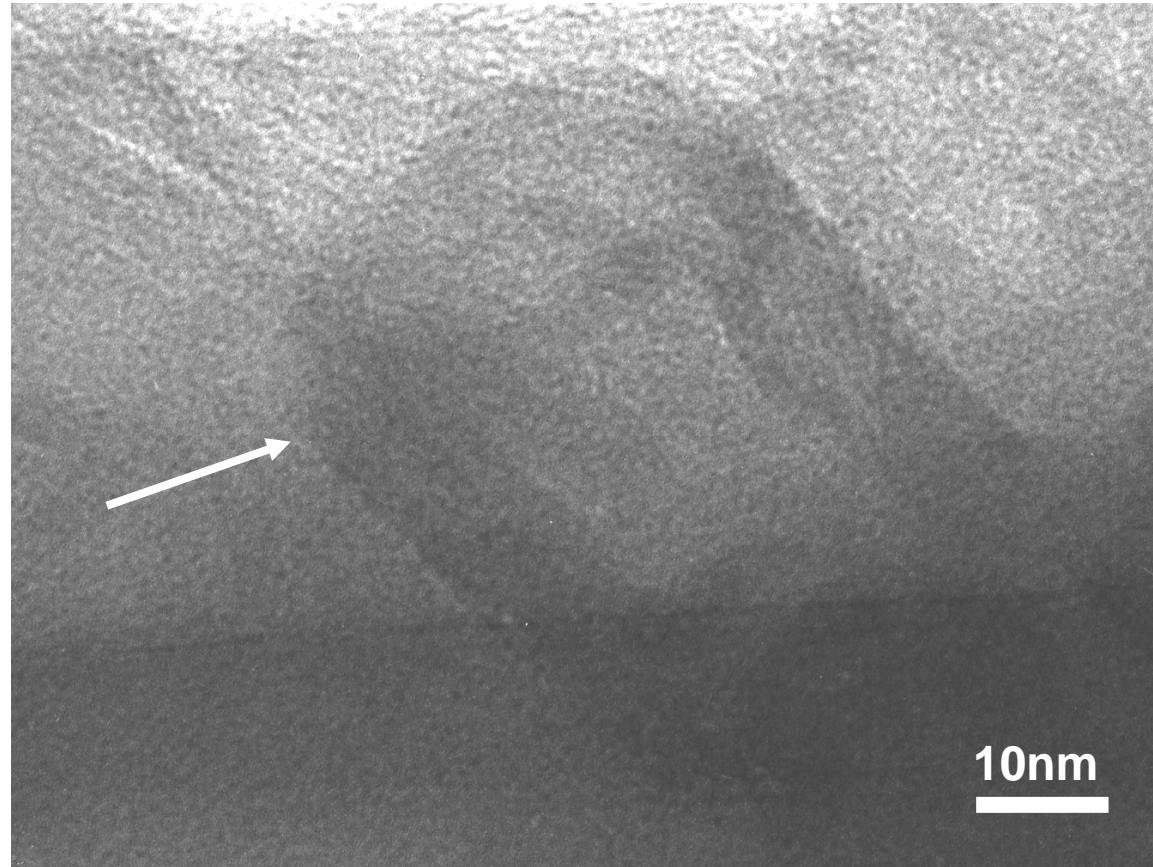


FIG.3. Kinoshita et al.

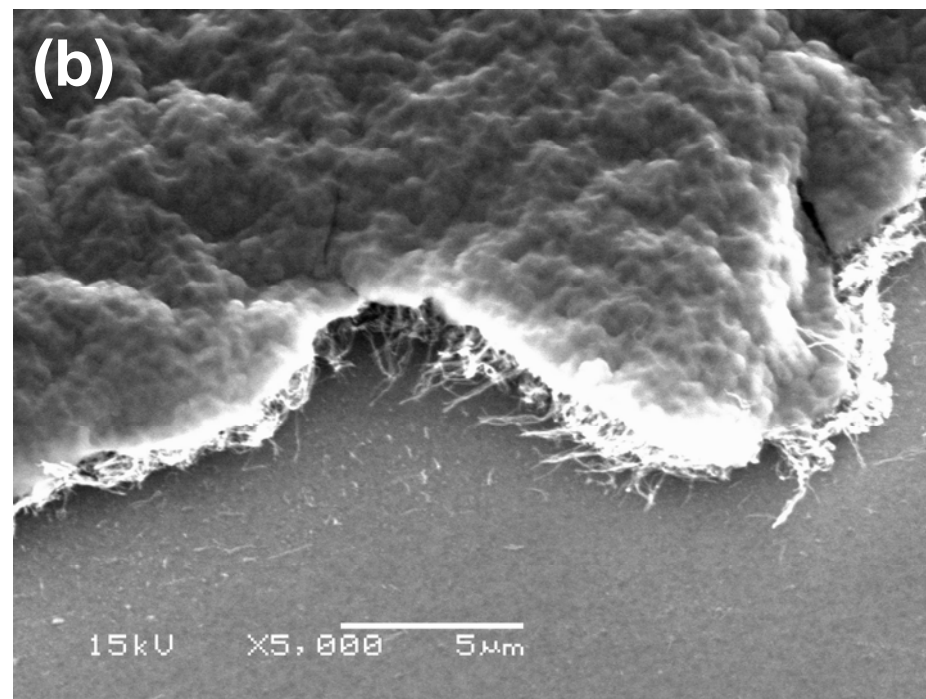
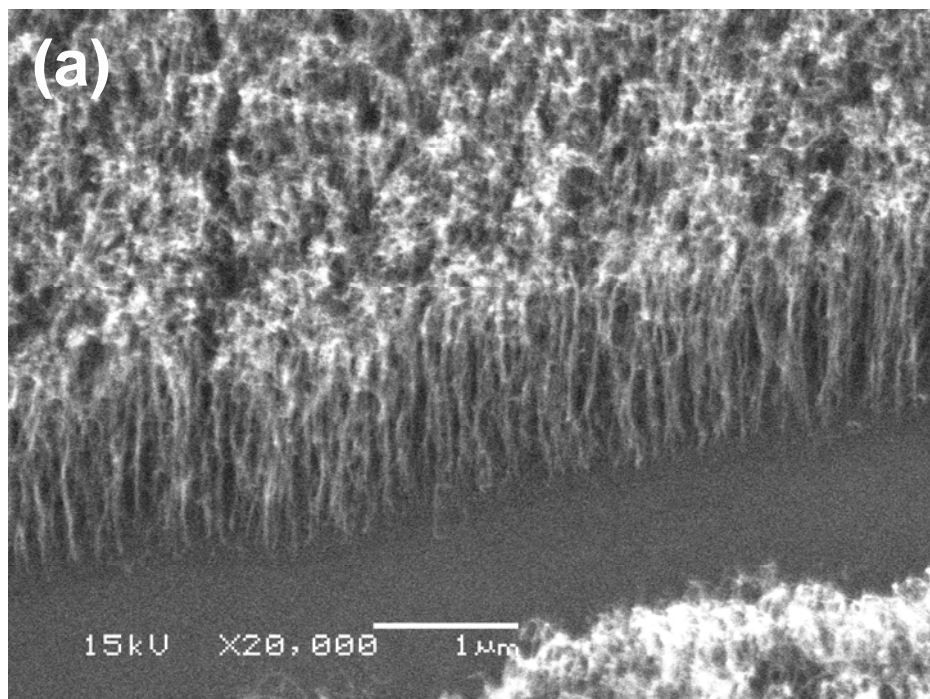


FIG.4. Kinoshita et al.

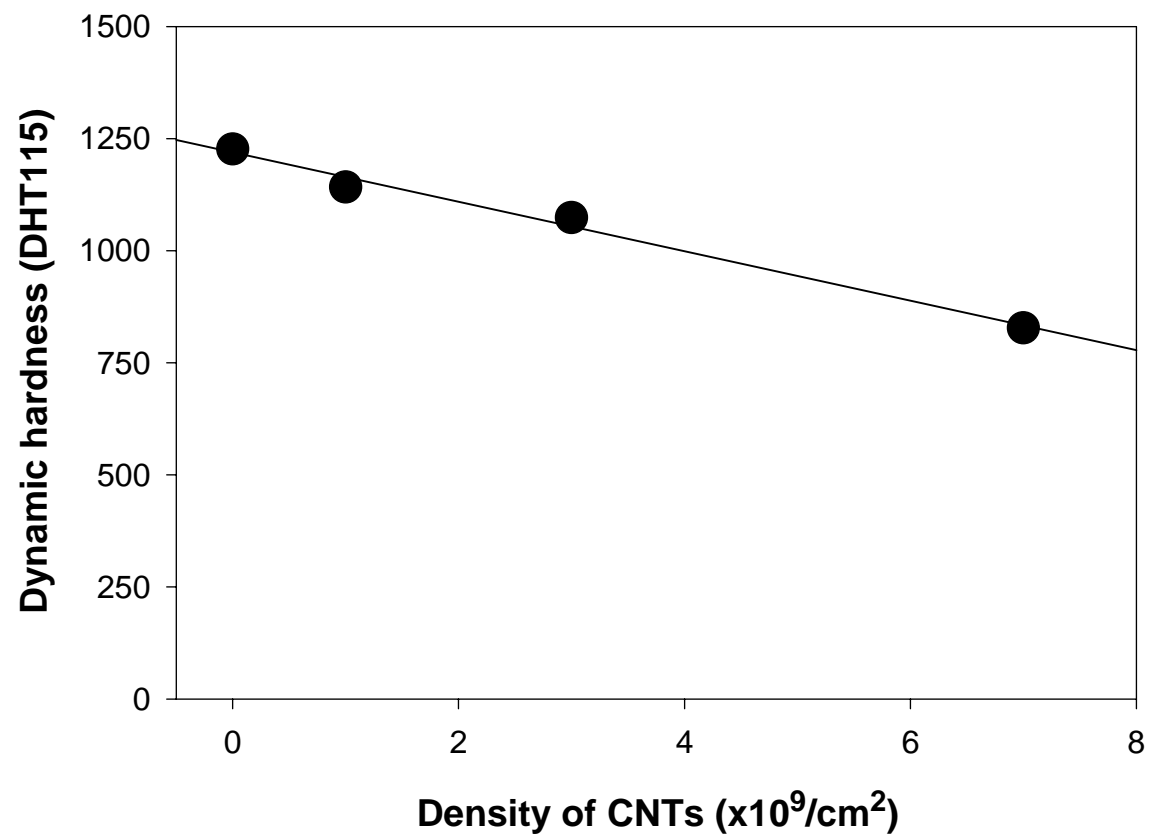


FIG.5. Kinoshita et al.

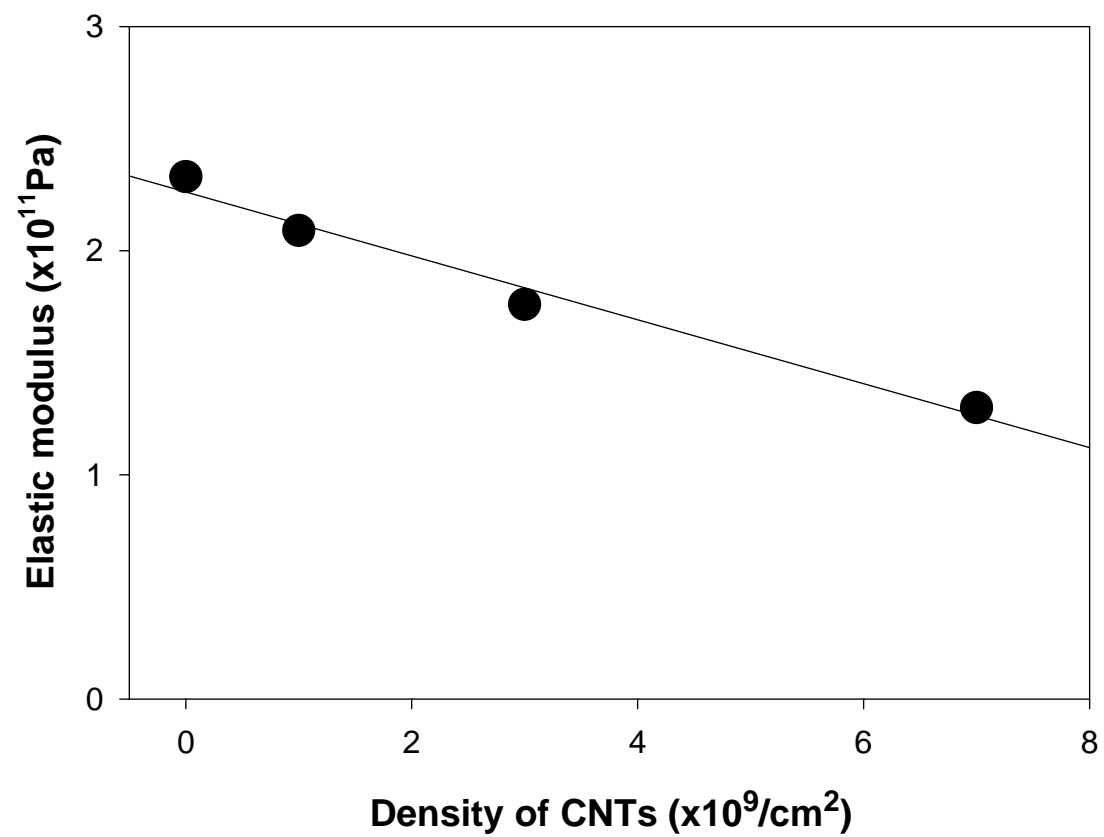


FIG.6. Kinoshita et al.

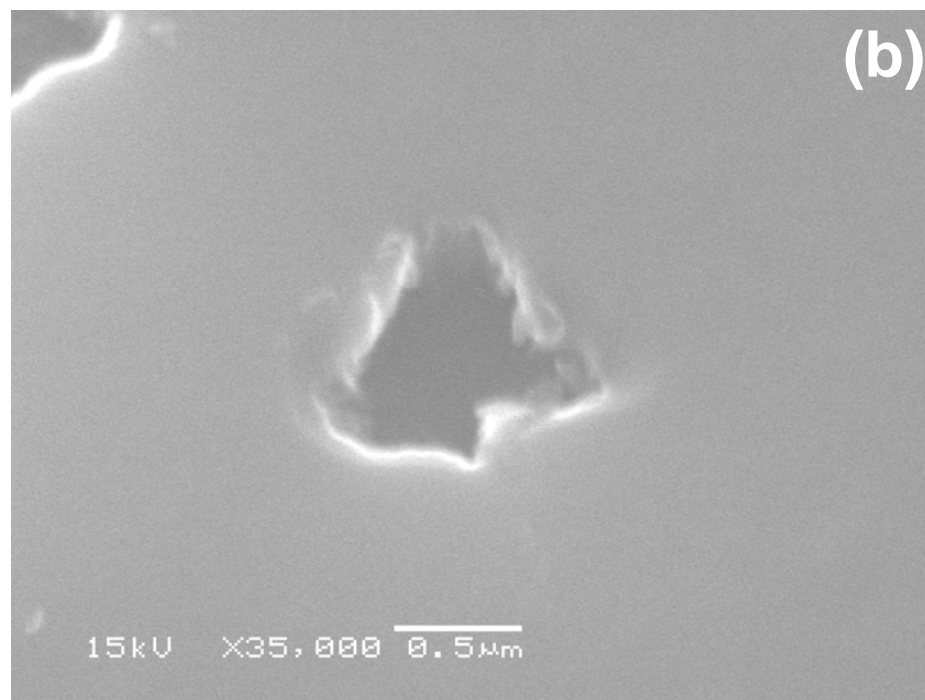
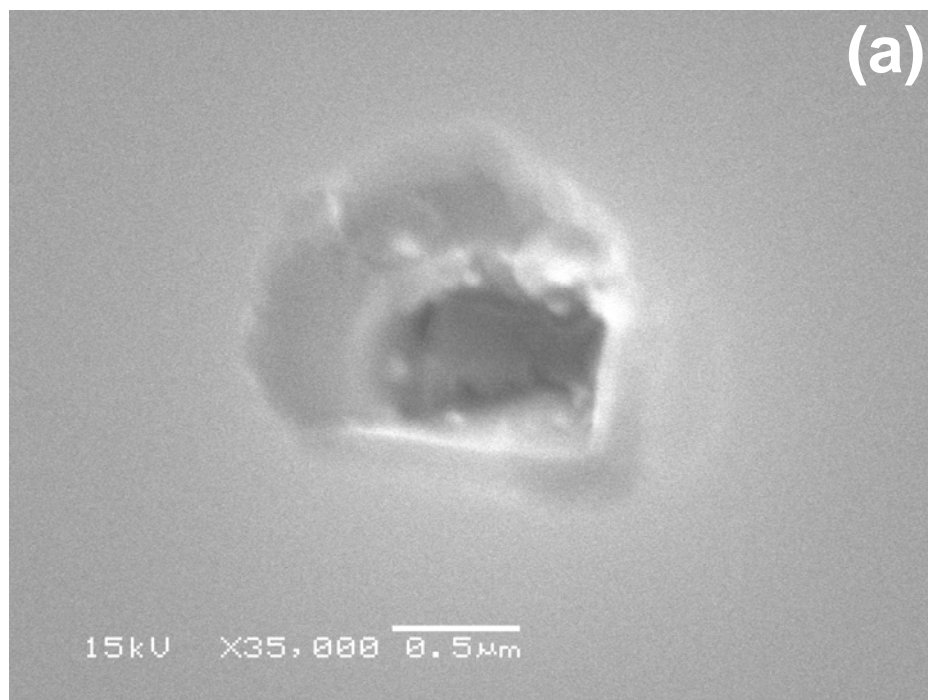


FIG.7. Kinoshita et al.

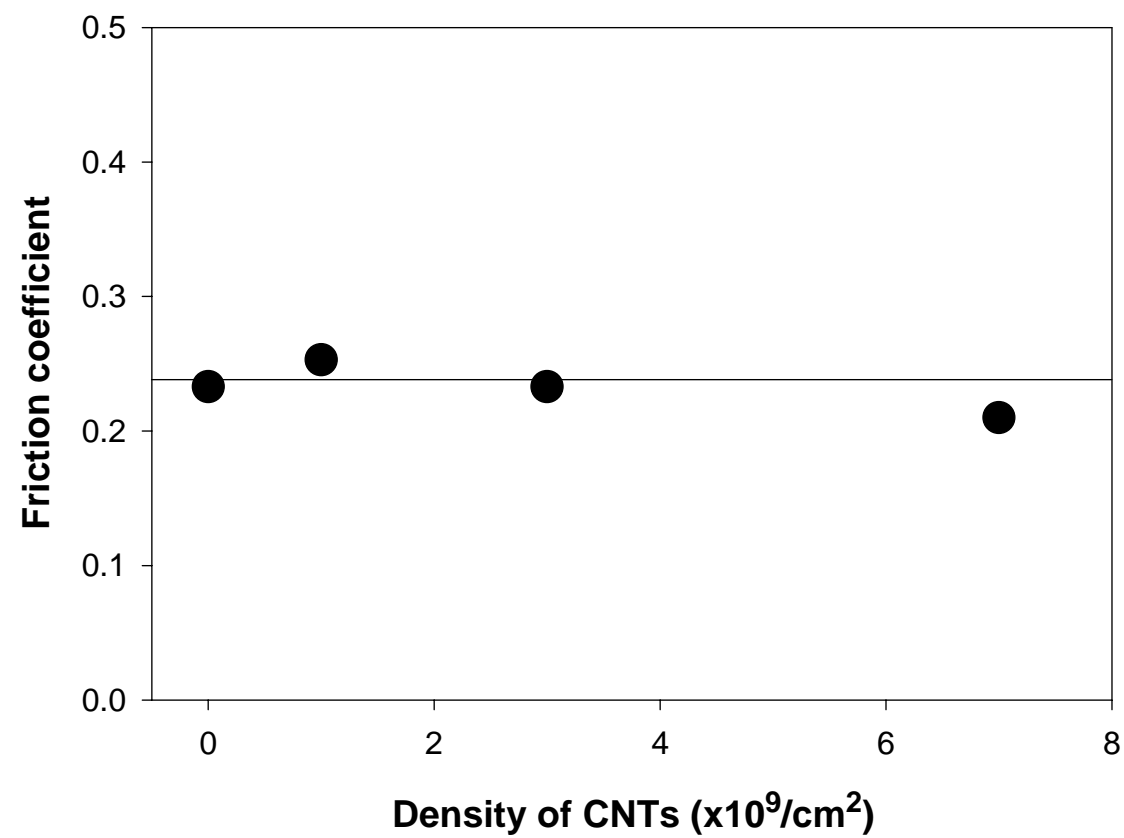


FIG.8. Kinoshita et al.